

# Permanent magnetic lattices for ultracold atoms and quantum degenerate gases

Saeed Ghanbari, Tien D Kieu, Andrei Sidorov and Peter Hannaford

Centre for Atom Optics and Ultrafast Spectroscopy and  
ARC Centre of Excellence for Quantum Atom Optics  
Swinburne University of Technology, Melbourne, Australia 3122

**Abstract.** We propose the use of periodic arrays of permanent magnetic films for producing magnetic lattices of microtraps for confining, manipulating and controlling small clouds of ultracold atoms and quantum degenerate gases. Using analytical expressions and numerical calculations we show that periodic arrays of magnetic films can produce one-dimensional (1D) and two-dimensional (2D) magnetic lattices with non-zero potential minima, allowing ultracold atoms to be trapped without losses due to spin flips. In particular, we show that two crossed layers of periodic arrays of parallel rectangular magnets plus bias fields, or a single layer of periodic arrays of square-shaped magnets with three different thicknesses plus bias fields, can produce 2D magnetic lattices of microtraps having non-zero potential minima and controllable trap depth. For arrays with micron-scale periodicity, the magnetic microtraps can have very large trap depths ( $\sim 0.5$  mK for the realistic parameters chosen for the 2D lattice) and very tight confinement.

## 1. Introduction

Periodic optical lattices produced by the interference of intersecting laser beams have been used extensively in recent years to confine, manipulate and control small clouds of ultracold atoms and Bose-Einstein condensates [1]. Such lattices are ideal tools for performing fundamental quantum physics experiments such as studies of low-dimensional quantum gases [2] and quantum tunnelling experiments including the BEC superfluid to Mott insulator quantum phase transition [3]. Optical lattices also have potential application in quantum information processing since they may provide storage registers for qubits based on neutral atoms [4, 5].

An alternative approach for producing periodic lattices for ultracold atoms is to use the magnetic potentials of periodic arrays of magnetic microtraps. Simple, one-dimensional (1D) magnetic lattices consisting of arrays of 2D traps or waveguides have been proposed [6] and constructed using current-carrying wires [7] or permanent magnetic structures [8, 9, 10] on ‘atom chips’, and two-dimensional (2D) lattices of magnetic microtraps produced by crossed arrays of current-carrying wires have been proposed [11, 12].

We have recently developed technology for producing high-quality magnetic microstructures based on permanent, perpendicularly magnetised magneto-optical  $Tb_6Gd_{10}Fe_{80}Co_4$  films [13]. These magnetic microstructures have been used to construct periodic grooved magnetic mirrors for ultracold atoms [13, 14], which in

the presence of bias magnetic fields can be transformed into a 1D magnetic lattice of 2D traps, and to produce atom chips for ultracold atoms and Bose-Einstein condensates [15]. The  $Tb_6Gd_{10}Fe_{80}Co_4$  magneto-optical films exhibit excellent magnetic properties for atom optics applications: they can be deposited with high perpendicular magnetic anisotropy; they have excellent magnetic homogeneity; and they can have high permanent magnetisation ( $4\pi M_z \sim 3.8 \text{ kG}$ ), large coercivity ( $H_c \sim 3 \text{ kOe}$ ) and relatively high Curie temperature ( $\sim 300^\circ\text{C}$ ).

In this paper we propose the use of periodic arrays of permanent magnetic films for producing magnetic lattices of microtraps for confining, manipulating and controlling small clouds of ultracold atoms and quantum degenerate gases. Using analytical expressions and numerical calculations we show that it is possible to produce 1D and 2D permanent magnetic lattices with non-zero potential minima in which ultracold atoms prepared in low magnetic field-seeking states can be trapped without losses due to Majorana spin flips. In particular, we show that two crossed separated layers of periodic arrays of parallel rectangular magnets plus bias magnetic fields, or a single layer of periodic arrays of square-shaped magnets having three different thicknesses plus bias fields, can produce 2D magnetic lattices of microtraps with non-zero potential minima and large and controllable trap depth and high trap frequency.

Magnetic lattices based on permanent magnetic films have potential advantages over optical lattices or magnetic lattices based on current-carrying wires that make them attractive for atom optics applications and compact integrated devices. They do not involve (high intensity) laser beams or any beam alignment, and there is no light scattering or decoherence due to spontaneous emission. They can produce highly stable reproducible potential wells with low technical noise. They can be produced with large trap depth and large magnetic field curvature, leading to very high trap frequencies, without heat dissipation, in contrast to current-carrying microwire devices. Using modern microtechnology, permanent magnetic lattices may be fabricated with a wide range of periods from about  $100 \mu\text{m}$  down to about  $1 \mu\text{m}$  and they can in principle involve variable spacing between the lattice sites or complex potential shapes at each lattice site. Finally, in magnetic lattices, only atoms in low magnetic field-seeking states are trapped and it should be possible to perform radiofrequency evaporative cooling *in situ* in the lattice, thereby allowing the study of very low temperature phenomena in lattices.

## 2. Analytical expressions for infinite magnetic lattices

### 2.1. Single infinite periodic array of magnets with bias fields

We consider first the simple case of a single infinite periodic array of parallel, rectangular, long magnets of thickness  $t$ , with periodicity  $a$  along the  $y$ -direction, perpendicular magnetisation  $M_z$ , and uniform bias magnetic fields  $B_{1x}$ ,  $B_{1y}$  and  $B_{1z}$  along the  $x$ -,  $y$ - and  $z$ -directions [figure 1(a)-(c)].

The components of the magnetic field at distance  $z$  from the bottom surface of the array of magnets [figure 1(b)] can be written as (using the results given in [16])

$$B_x = B_{1x} \quad (1a)$$

$$B_y = B_0[(1 - e^{-kt})e^{-k[z-(s+t)]} \sin(ky) - \frac{1}{3}(1 - e^{-3kt})e^{-3k[z-(s+t)]} \sin(3ky) + \dots] + B_{1y} \quad (1b)$$

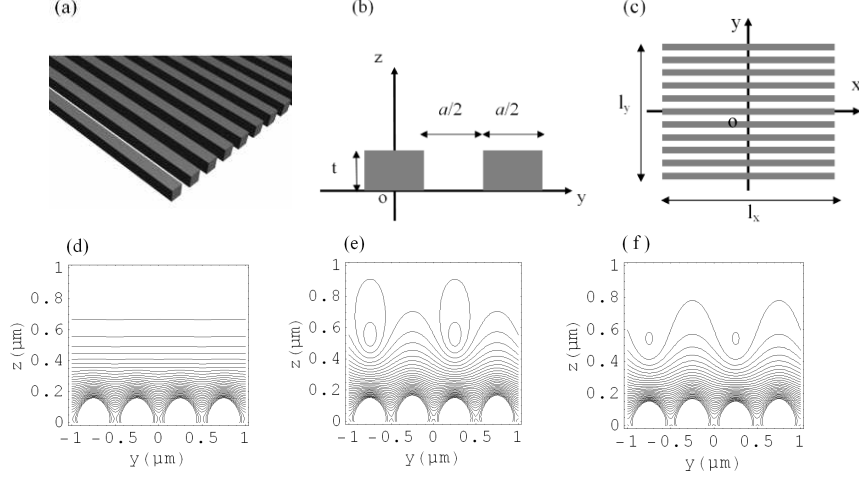


**Figure 1.** (a-c) Single periodic array of parallel, rectangular magnets with perpendicular magnetization. (d-f) Contour plots of the magnitude of the magnetic field in the central region in the  $yoz$  plane without bias fields (d), with a bias field  $B_{1y} = -15$  G along the  $y$ -direction (e), and with bias fields  $B_{1x} = -20$  G,  $B_{1y} = -15$  G and  $B_{1z} = -0.09$  G along the  $x$ -,  $y$ - and  $z$ -directions. For this calculation, the number of magnets  $n_r = 1001$ ,  $t = 0.05$   $\mu\text{m}$ ,  $a = 1$   $\mu\text{m}$ ,  $l_x = 1000.5$   $\mu\text{m}$ , and  $4\pi M_z = 3.8$  kG. The spacing between the contour lines is 7 G.

$$B_z = B_0[(1 - e^{-kt})e^{-k[z-(s+t)]} \cos(ky) - \frac{1}{3}(1 - e^{-3kt})e^{-3k[z-(s+t)]} \cos(3ky) + \dots] + B_{1z} \quad (1c)$$

where the decay constant  $k = 2\pi/a$ ,  $B_0 = 4M_z$  (Gaussian units), and the factors  $(1 - e^{-kt})$ ,  $(1 - e^{-3kt})$ ,  $\dots$  account for the finite thickness  $t$  of the magnets.

For distances from the surface which are large compared with  $a/4\pi$ , the higher order spatial harmonics in (1b) and (1c) will have decayed away, and (1a)-(1c) reduce to

$$B_x = B_{1x} \quad (2a)$$

$$B_y = B_{0y} \sin(ky)e^{-kz} + B_{1y} \quad (2b)$$

$$B_z = B_{0y} \cos(ky)e^{-kz} + B_{1z} \quad (2c)$$

where  $B_{0y} = B_0(1 - e^{-kt})e^{kt}$ . The magnitude of the magnetic field is then given by

$$B(y, z) = \left\{ B_{1x}^2 + B_{1y}^2 + B_{1z}^2 + 2[B_{0y}B_{1y} \sin(ky) + B_{0y}B_{1z} \cos(ky)]e^{-kz} + B_{0y}^2 e^{-2kz} \right\}^{\frac{1}{2}} \quad (3)$$

The effect of the bias fields  $B_{1y}$  and  $B_{1z}$  is essentially the same; so we set  $B_{1z} = 0$ . This results in a 1D periodic magnetic lattice of 2D magnetic traps with *non-zero* potential minima, given by

$$B_{min} = |B_{1x}| \quad (4)$$

which are located at

$$y_{min} = \left(n_y + \frac{1}{4}\right) a \quad (5a)$$

$$z_{min} = \frac{a}{2\pi} \ln \left( \frac{B_{0y}}{|B_{1y}|} \right) \quad (5b)$$

where  $n_y = 0, \pm 1, \pm 2, \dots$  represents the trap number in the  $y$ -direction. The barrier heights in the  $y$ - and  $z$ -directions are given by

$$\Delta B^y = B_{max}^y - B_{min} = (B_{1x}^2 + 4B_{1y}^2)^{\frac{1}{2}} - |B_{1x}| \quad (6a)$$

$$\Delta B^z = B_{max}^z - B_{min} = (B_{1x}^2 + B_{1y}^2)^{\frac{1}{2}} - |B_{1x}| \quad (6b)$$

The curvatures of the magnetic field at the centre of the 2D magnetic traps and the trap frequencies in the  $y$ - and  $z$ -directions are given by

$$\frac{\partial^2 B}{\partial y^2} = \frac{\partial^2 B}{\partial z^2} = \frac{4\pi^2}{a^2} \frac{B_{1y}^2}{|B_{1x}|} \quad (7)$$

$$\omega_y = \omega_z = \frac{2\pi}{a} \left( \frac{m_F g_F \mu_B}{m |B_{1x}|} \right)^{\frac{1}{2}} |B_{1y}| \quad (8)$$

where  $m_F$  is the magnetic quantum number of the hyperfine state  $F$ ,  $g_F$  is the Landé g-factor,  $\mu_B$  is the Bohr magneton and  $m$  is the atomic mass. Equations (5b) and (8) are the same as given in [9].

*2.1.1. No bias fields* For the case of no bias fields, (3) reduces to

$$B(z) = B_{0y} e^{-kz} \quad (9)$$

Under these conditions the magnitude of the magnetic field falls off exponentially with distance  $z$  from the surface. This configuration represents the familiar case of a grooved magnetic mirror for slowly moving atoms in low magnetic field-seeking states [14].

*2.1.2. Single bias field  $B_{1y}$*  For the case of a single bias field  $B_{1y}$ , (3) becomes

$$B(y, z) = \left\{ B_{1y}^2 + 2B_{0y}B_{1y} \sin(ky) e^{-kz} + B_{0y}^2 e^{-2kz} \right\}^{\frac{1}{2}} \quad (10)$$

The magnitude of the magnetic field develops corrugations with period  $a$  in the  $y$ -direction, and 2D magnetic traps with  $B_{min} = 0$  appear in the potentials above the surface. This configuration, involving a single bias field, may be used as a spatial diffraction grating for slowly moving atoms [17, 18, 19, 20], but is not useful as a magnetic lattice for ultracold atoms because of the zero potential minima.

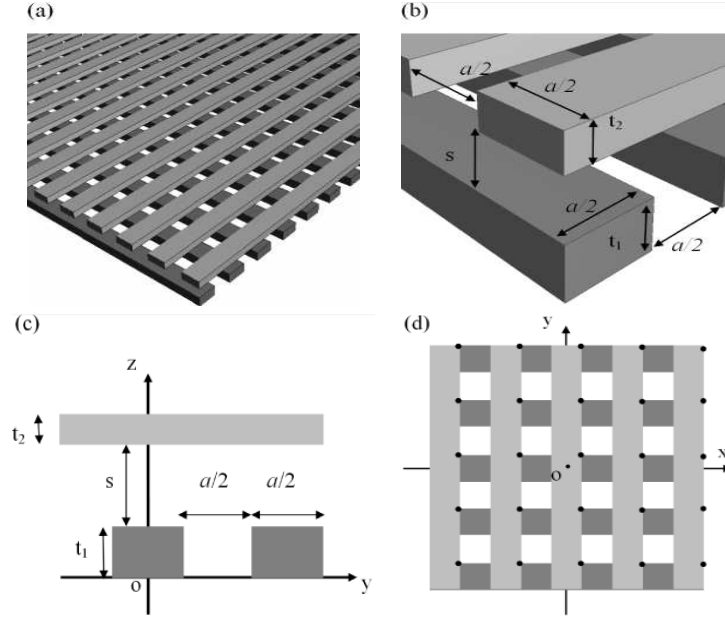


**Figure 2.** Periodic array consisting of two crossed layers of parallel, rectangular permanent magnets with perpendicular magnetisation. In (d) the locations of the central minima in the  $xoy$  plane are shown for a symmetrical magnetic lattice with bias fields  $B_{1x} = -4.08$  G,  $B_{1y} = -6.05$  G and  $B_{1z} = -0.69$  G and other parameters as given in table 1, column 3.

**Table 1.** Input parameters for (1) two crossed layers of periodic arrays of rectangular magnets (figure 2), and (2) a single layer of square magnets with three thicknesses (figure 7).

Parameter	Definition	Configuration (1)	Configuration (2)
$n_r$ or $n_{sq}$	Number of rectangular magnets or square magnets in $x$ - or $y$ -direction	$n_r = 1001$	$n_{sq} = 401$
$a$ ( $\mu m$ )	Period of magnetic lattice	1.000	1.000
$l_x = l_y$ ( $\mu m$ )	Length of magnets or magnetic array along $x$ or $y$	1000.5	200.5
$s$ ( $\mu m$ )	Separation of magnetic layers	0.100	
$t_1$ ( $\mu m$ )	Thickness of magnetic film (first)	0.322	0.100
$t_2$ ( $\mu m$ )	Thickness of magnetic film (second)	0.083	0.120
$t_3$ ( $\mu m$ )	Thickness of magnetic film (third)		0.220
$4\pi M_z$ (G)	Magnetisation along $z$	3800	3800
$B_{1x}$ (G)	Bias magnetic field along $x$	-4.08	-5.00
$B_{1y}$ (G)	Bias magnetic field along $y$	-6.05	-4.22
$B_{1z}$ (G)	Bias magnetic field along $z$	-0.69	-1.87

## 2.2. Two crossed layers of infinite periodic arrays of magnets with bias fields

We now consider a configuration consisting of two crossed, separated, infinite periodic arrays of parallel, rectangular, long magnets with perpendicular magnetization  $M_z$  and uniform bias fields  $B_{1x}$ ,  $B_{1y}$  and  $B_{1z}$  along the  $x$ -,  $y$ - and  $z$ -directions (figure 2). The bottom array has periodicity  $a$  along the  $y$ -direction and the top array has periodicity  $a$  along the  $x$ -direction. The two arrays are separated by a distance  $s$  and the magnets in the bottom array have thickness  $t_1$  while those in the top array have thickness  $t_2$  [see figure 2(b)]. This configuration of crossed permanent magnets with bias fields has similarities to the crossed current-carrying wire configurations proposed by Yin *et al* [11] and by Grabowski and Pfau [12]. The components of the magnetic field for distances from the top surface which are large compared with  $a/4\pi$  are given by

$$B_x = B_{0x} \sin(kx)e^{-kz} + B_{1x} \quad (11a)$$

$$B_y = B_{0y} \sin(ky)e^{-kz} + B_{1y} \quad (11b)$$

$$B_z = [B_{0x} \cos(kx) + B_{0y} \cos(ky)]e^{-kz} + B_{1z} \quad (11c)$$

where

$$B_{0x} = B_0(1 - e^{-kt_2})e^{k(s+t_1+t_2)} \quad (12a)$$

$$B_{0y} = B_0(1 - e^{-kt_1})e^{kt_1} \quad (12b)$$

The magnitude of the magnetic field above the crossed magnetic arrays is then

$$\begin{aligned} B(x, y, z) = & \left\{ B_{1x}^2 + B_{1y}^2 + B_{1z}^2 \right. \\ & + 2[B_{0x}B_{1x} \sin(kx) + B_{0y}B_{1y} \sin(ky) \\ & + B_{0x}B_{1z} \cos(kx) + B_{0y}B_{1z} \cos(ky)]e^{-kz} \\ & \left. + [B_{0x}^2 + B_{0y}^2 + 2B_{0x}B_{0y} \cos(kx) \cos(ky)]e^{-2kz} \right\}^{\frac{1}{2}} \quad (13) \end{aligned}$$

*2.2.1. Two bias fields  $B_{1x}$  and  $B_{1y}$*  For the case of two bias fields  $B_{1x}$  and  $B_{1y}$ , (13) becomes

$$\begin{aligned} B(x, y, z) = & \left\{ B_{1x}^2 + B_{1y}^2 \right. \\ & + 2[B_{0x}B_{1x} \sin(kx) + B_{0y}B_{1y} \sin(ky)]e^{-kz} \\ & \left. + [B_{0x}^2 + B_{0y}^2 + 2B_{0x}B_{0y} \cos(kx) \cos(ky)]e^{-2kz} \right\}^{\frac{1}{2}} \quad (14) \end{aligned}$$

This configuration results in a 2D periodic lattice of magnetic traps with *non-zero* potential minima given by

$$B_{min} = \frac{|B_{0x}B_{1y} - B_{0y}B_{1x}|}{(B_{0x}^2 + B_{0y}^2)^{\frac{1}{2}}} \quad (15)$$

2.2.2. *Symmetrical magnetic lattice with bias fields  $B_{1x}$  and  $B_{1y}$*  To produce a symmetrical magnetic lattice the amplitude of the oscillating magnetic field produced by the bottom magnetic array in the  $y$ -direction needs to equal the amplitude of the oscillating magnetic field produced by the top array in the  $x$ -direction. To satisfy this condition we impose the constraint

$$B_{0x}B_{1x} = B_{0y}B_{1y} \quad (16a)$$

or

$$B_{1y} = c_0 B_{1x} \quad (16b)$$

where

$$c_0 = \frac{B_{0x}}{B_{0y}} = \left( \frac{e^{kt_2} - 1}{1 - e^{-kt_1}} \right) e^{ks} \quad (17)$$

is a dimensionless constant which only involves geometrical constants  $a, s, t_1$  and  $t_2$  of the magnetic array. The magnetic traps then have non-zero potential minima given by

$$B_{min} = c_1 |B_{1x}| \quad (18)$$

which are located at

$$x_{min} = \left( n_x + \frac{1}{4} \right) a, \quad n_x = 0, \pm 1, \pm 2, \dots \quad (19a)$$

$$y_{min} = \left( n_y + \frac{1}{4} \right) a, \quad n_y = 0, \pm 1, \pm 2, \dots \quad (19b)$$

$$z_{min} = \frac{a}{2\pi} \ln \left( \frac{c_2 B_{0x}}{|B_{1x}|} \right) \quad (19c)$$

where  $c_1$  and  $c_2$  are dimensionless constants which may be expressed in terms of the constant  $c_0 = B_{0x}/B_{0y}$

$$c_1 = \frac{|1 - c_0^2|}{(1 + c_0^2)^{\frac{1}{2}}} \quad (20a)$$

$$c_2 = \frac{1}{2} \left( 1 + \frac{1}{c_0^2} \right) \quad (20b)$$

In order to have non-zero potential minima above the surface of the top array, we have the following constraints

$$c_2 B_{0x} > |B_{1x}| > 0, \quad c_0 c_2 B_{0y} > |B_{1y}| > 0, \quad B_{0x} \neq B_{0y} \quad (21)$$

The curvatures of the magnetic field at the centre of the traps and the trap frequencies (for the case of a harmonic potential) in the three directions are given by

$$\frac{\partial^2 B}{\partial x^2} = \frac{\partial^2 B}{\partial y^2} = \frac{1}{2} \frac{\partial^2 B}{\partial z^2} = \frac{4\pi^2 c_3}{a^2} |B_{1x}| \quad (22)$$

$$\omega_x = \omega_y = \frac{\omega_z}{\sqrt{2}} = \frac{2\pi}{a} \left( \frac{m_F g_F \mu_B c_3}{m} \right)^{\frac{1}{2}} |B_{1x}|^{\frac{1}{2}} \quad (23)$$

The potential barrier heights in the three directions are given by

$$\Delta B^x = \Delta B^y = c_4 |B_{1x}| \quad (24a)$$

$$\Delta B^z = c_5 |B_{1x}| \quad (24b)$$

$c_3$ ,  $c_4$  and  $c_5$  are dimensionless constants which may be expressed in terms of  $c_0$

$$c_3 = \frac{2c_0^2}{(1+c_0^2)^{\frac{1}{2}}|1-c_0^2|} \quad (25a)$$

$$c_4 = \left(1 + c_0^2 + \frac{4c_0^2}{1+c_0^2}\right)^{\frac{1}{2}} - \frac{|1-c_0^2|}{(1+c_0^2)^{\frac{1}{2}}} \quad (25b)$$

$$c_5 = (1+c_0^2)^{\frac{1}{2}} \quad (25c)$$

The barrier heights in the  $x$ -,  $y$ - and  $z$ -directions vary with  $z_{min}$  as

$$\Delta B^x = \Delta B_0^x e^{-k(z_{min}-z_{min0})} = \Delta B^y = \Delta B_0^y e^{-k(z_{min}-z_{min0})} \quad (26a)$$

$$\Delta B^z = \Delta B_0^z e^{-k(z_{min}-z_{min0})} \quad (26b)$$

where

$$\Delta B_0^x = \Delta B_0^y = c_1 c_4 B_{0x} e^{-kz_{min0}} \quad (27a)$$

$$\Delta B_0^z = c_1 c_5 B_{0x} e^{-kz_{min0}} \quad (27b)$$

If  $B_{1x}$  and  $B_{1y}$  are not subject to the constraint (16a) we have  $\Delta B^x \neq \Delta B^y$ . In some experiments, e.g., in studies of quantum tunnelling between lattice sites, it may be useful to be able to have different barrier heights along different axes.

*2.2.3. Three bias fields  $B_{1x}$ ,  $B_{1y}$  and  $B_{1z}$*  For the case of three bias fields  $B_{1x}$ ,  $B_{1y}$  and  $B_{1z}$ , the magnitude of the magnetic field is given by (13). The analytical expressions for  $B_{min}$ ,  $x_{min}$ ,  $y_{min}$  and  $z_{min}$  in this case become very complex and we resort to numerical evaluation of (13) to determine these quantities. Moreover, the condition for a symmetrical magnetic lattice in the case  $B_z \neq 0$  imposes the constraints

$$B_{0x} = B_{0y}, \quad B_{1x} = B_{1y} \quad (28)$$

and under such conditions,  $B_{min} = 0$ . Thus in the case of an *infinite* symmetrical magnetic lattice with three bias fields,  $B_{1x}$ ,  $B_{1y}$  and  $B_{1z}$ , it is not possible to have non-zero potential minima.

Nevertheless, we find that in the case of a *finite* magnetic lattice it is useful to be able to apply a bias field  $B_{1z}$  in order to compensate for the asymmetry introduced into the lattice by end-effects [21] associated with the finite number of magnets in the array (see section 3).

### 3. Numerical calculations for finite magnetic lattices

To calculate magnetostatic potentials for arbitrary configurations, including finite periodic arrays of magnets of finite length and arbitrary cross section, the software package Radia [22] interfaced to Mathematica was used. Radia was also used to test various proposed configurations of permanent magnets that might support periodic arrays of microtraps with non-zero potential minima based on symmetry arguments.



### 3.1. Single finite periodic array of magnets with bias fields

Figure 1(d) shows a numerical calculation of the magnetic field versus distance in the  $y$ -direction for the central region of a single finite array of  $n_r = 1001$  rectangular magnets, using the parameters  $a = 1 \mu m$ ,  $t = 0.050 \mu m$ ,  $l_x = 1000.5 \mu m$  and  $4\pi M_z = 3.8 kG$  (corresponding to the magnetization of our perpendicularly magnetized  $Tb_6Gd_{10}Fe_{80}Co_4$  magneto-optical films [13, 15]) and with *no bias* magnetic fields. Corrugations corresponding to the third-order spatial harmonic with period  $a/2$  [16] [see (1b) and (1c)] can be seen at distances very close ( $\ll a/4\pi$ ) to the surface. At large distances, there are small residual corrugations with period  $a$ , which are due to ‘end effects’ [21] associated with the finite number (1001) of magnets in the array. This configuration may be used as a magnetic mirror for slowly moving atoms [14].

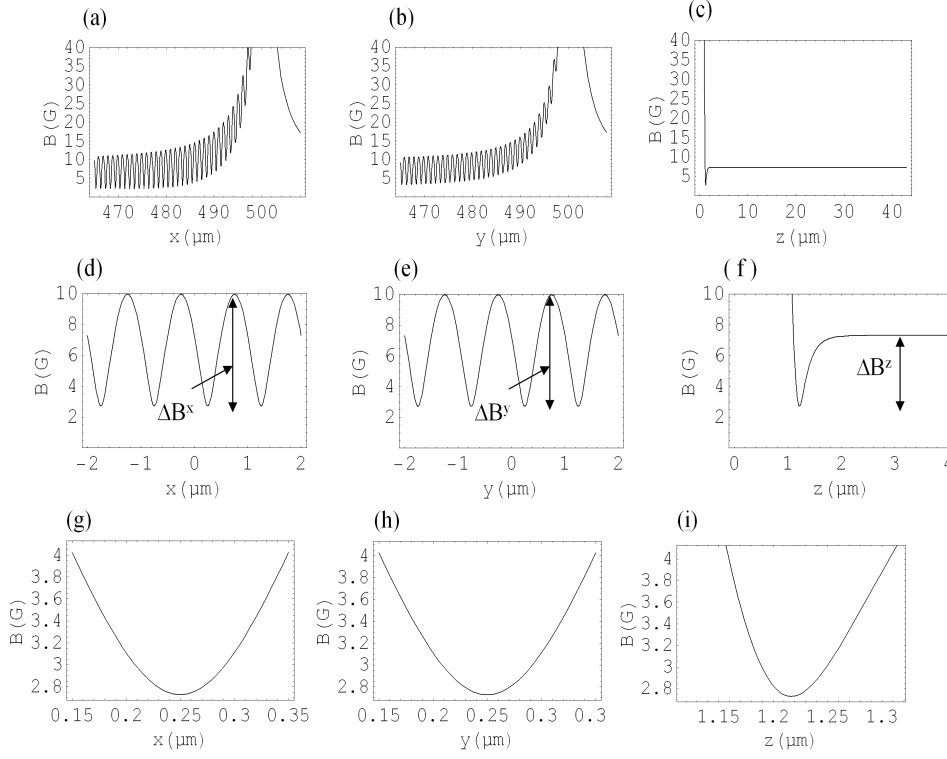
Figure 1(e) shows the effect of adding a bias field  $B_{1y} = -15 G$ . The magnitude of the magnetic field develops large corrugations with period  $a$  in the  $y$ -direction, and 2D magnetic traps with  $B_{min} = 0$  appear in the potentials at  $z_{min} = 0.540 \mu m$ . This configuration may be used as a spatial diffraction grating [17, 18, 19, 20] for slowly moving atoms.

Figure 1(f) shows the effect of having bias fields  $B_{1x} = -20 G$ ,  $B_{1y} = -15 G$  and  $B_{1z} = -0.09 G$ . The small value of  $B_{1z}$  was chosen in order to compensate for asymmetry introduced into the lattice by end-effects [21] associated with the finite number of magnets (1001) in the array. Non-zero potential minima with  $B_{min} = |B_{1x}| = 20 G$  appear in the potentials at  $z_{min} = 0.540 \mu m$ . This configuration may be used as a 1D periodic lattice of 2D magnetic traps or waveguides for slowly moving atoms. Relatively large values of  $B_{1x}$  and  $B_{1y}$  were used in this calculation so that the magnetic traps are sufficiently deep to be seen in the contour plot. In practice smaller values would normally be used. For example, if we use  $B_{1x} = -2.73 G$ ,  $B_{1y} = -0.22 G$  and  $B_{1z} = -0.09 G$ , non-zero potential minima with  $B_{min} = |B_{1x}| = 2.73 G$  appear in the potentials at  $z_{min} = 1.216 \mu m$ .

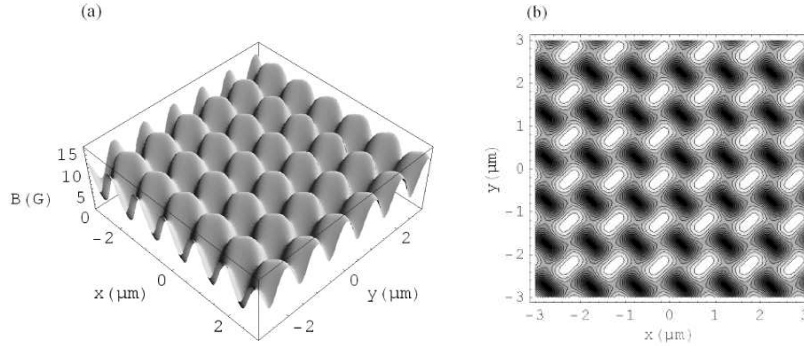
### 3.2. Two crossed layers of finite periodic arrays of magnets with bias fields

Figure 3 shows a numerical calculation of the magnetic field versus distance in the  $x$ -,  $y$ - and  $z$ -directions of a *finite* array consisting of two crossed layers of periodic arrays of parallel rectangular magnets. The parameters are  $n_r = 1001$ ,  $a = 1 \mu m$ ,  $s = 0.1 \mu m$ ,  $t_1 = 0.322 \mu m$  (bottom layer),  $t_2 = 0.083 \mu m$  (top layer),  $4\pi M_z = 3.8 kG$ ,  $B_{1x} = -4.08 G$ ,  $B_{1y} = -6.05 G$  and  $B_{1z} = -0.69 G$  (see table 1). The values of  $B_{1x}$ ,  $B_{1y}$ ,  $s$ ,  $t_1$  and  $t_2$  satisfy the condition for a symmetrical *infinite* magnetic lattice with two bias fields [equations (16a) or (16b)], while the value of  $B_{1z}$  was adjusted to compensate for asymmetry introduced into the lattice by ‘end-effects’ associated with the finite number (1001) of magnets in the array (see section 2.2.3). The peaks at the ends of the array [figure 3(a) and (b)] also arise from end-effects. The potential of the microtraps is close to harmonic in the region near the bottom of the traps [figure 3 (g)-(i)].

Figure 4 shows a 3D plot and a contour plot of the magnetic field in the plane  $z = z_{min}$  for the two crossed-layer structure of parallel magnets. The parameters used in this calculation (table 1, column 3) lead to  $(n_r - 1)^2 = 10^6$  magnetic microtraps with  $B_{min} = 2.73 G$  at the *central* minimum, which is located at  $d = 0.712 \mu m$  from the top surface, and magnetic field barrier heights  $\Delta B^x = B_{max}^x - B_{min} = \Delta B^y = 7.23 G$  and  $\Delta B^z = 4.57 G$ . The potential minima in the outer regions of the array have slightly



**Figure 3.** Magnetic field produced by a periodic array consisting of two crossed layers of parallel rectangular magnets. (a) Near the edge in the  $x$  direction, (b) near the edge in the  $y$ -direction, and (c) in the  $z$  direction, for parameters given in table 1, column 3. Curves (d)-(f) show the magnetic field in the central region of the lattice with the abscissa expanded. Curves (g)-(i) show the magnetic field in the central region of the lattice plotted (g) along a line ( $y = y_{min}$ ,  $z = z_{min}$ ) parallel to the  $x$ -axis, (h) along a line ( $x = x_{min}$ ,  $z = z_{min}$ ) parallel to the  $y$ -axis, and (i) along a line ( $x = x_{min}$ ,  $y = y_{min}$ ) parallel to the  $z$ -axis.



**Figure 4.** Magnetic field in the plane  $z = z_{min}$  for a periodic array consisting of two crossed layers of parallel rectangular magnets. (a) 3D plot, and (b) contour plot, for parameters given in table 1, column 3.

**Table 2.** Parameters calculated numerically using Radia (columns 3 and 6) and using the analytical formulae (columns 4 and 5) for the input parameters in table 1 for (1) two crossed layers of periodic arrays of rectangular magnets (figure 2), and (2) a single layer of square magnets with three thicknesses (figure 7).

Parameter	Definition	Config.(1)			Config.(2)
		Numerical	Analytical		Numerical
			$B_{1z} = 0$	$B_{1z} = -0.69$ (G)	
$x_{min}$ ( $\mu m$ )	$x$ co-ordinate of potential minimum	0.250	0.250	0.184	0.250
$y_{min}$ ( $\mu m$ )	$y$ co-ordinate of potential minimum	0.250	0.250	0.294	0.250
$z_{min}$ ( $\mu m$ )	$z$ co-ordinate of potential minimum	1.216	1.216	1.206	0.952
$d$ ( $\mu m$ )	Distance of central minimum from surface	0.712	0.712	0.702	0.732
$B_{min}$ (G)	Magnetic field at potential minimum	2.73	2.73	2.64	1.10
$\frac{\partial^2 B}{\partial x^2}$ ( $\frac{G}{cm^2}$ )	Curvature of $B$ along $x$	$3.32 \times 10^{10}$	$3.31 \times 10^{10}$	$3.77 \times 10^{10}$	$7.52 \times 10^{10}$
$\frac{\partial^2 B}{\partial y^2}$ ( $\frac{G}{cm^2}$ )	Curvature of $B$ along $y$	$3.32 \times 10^{10}$	$3.32 \times 10^{10}$	$3.77 \times 10^{10}$	$7.52 \times 10^{10}$
$\frac{\partial^2 B}{\partial z^2}$ ( $\frac{G}{cm^2}$ )	Curvature of $B$ along $z$	$6.64 \times 10^{10}$	$6.64 \times 10^{10}$	$6.98 \times 10^{10}$	$1.50 \times 10^{11}$
$\Delta B^x$ (G)	Magnetic barrier height along $x$	7.22	7.22	8.01	8.10
$\Delta B^y$ (G)	Magnetic barrier height along $y$	7.23	7.23	7.78	8.09
$\Delta B^z$ (G)	Magnetic barrier height along $z$	4.57	4.57	4.69	5.45

**Table 3.** Parameters calculated numerically using Radia for input parameters in table 1 for  $^{87}\text{Rb}$   $F = 2$ ,  $m_F = +2$  atoms trapped in a magnetic lattice consisting of (1) two crossed layers of periodic arrays of rectangular magnets (figure 2), and (2) a single layer of square magnets with three thicknesses (figure 7).

Parameter	Definition	Configuration (1)	Configuration (2)
$U_{min}/k_B$ ( $\mu K$ )	Energy of minimum of potential	183	74
$\Delta U^x/k_B$ ( $\mu K$ )	Potential barrier height along $x$	485	544
$\Delta U^y/k_B$ ( $\mu K$ )	Potential barrier height along $y$	486	544
$\Delta U^z/k_B$ ( $\mu K$ )	Potential barrier height along $z$	307	383
$\omega_x/2\pi$ (kHz)	Trap frequency along $x$	232	350
$\omega_y/2\pi$ (kHz)	Trap frequency along $y$	233	350
$\omega_z/2\pi$ (kHz)	Trap frequency along $z$	329	494
$\hbar\omega_x/k_B$ ( $\mu K$ )	Level spacing along $x$	11	17
$\hbar\omega_y/k_B$ ( $\mu K$ )	Level spacing along $y$	11	17
$\hbar\omega_z/k_B$ ( $\mu K$ )	Level spacing along $z$	16	24

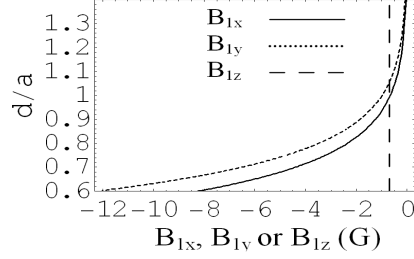


**Figure 5.** Distance of the central minimum from the surface  $d = z_{min} - (t_1 + t_2 + s)$  (in units of  $a$ ) versus bias fields  $B_{1x}$ ,  $B_{1y}$  or  $B_{1z}$ , for the parameters given in table 1, column 3.

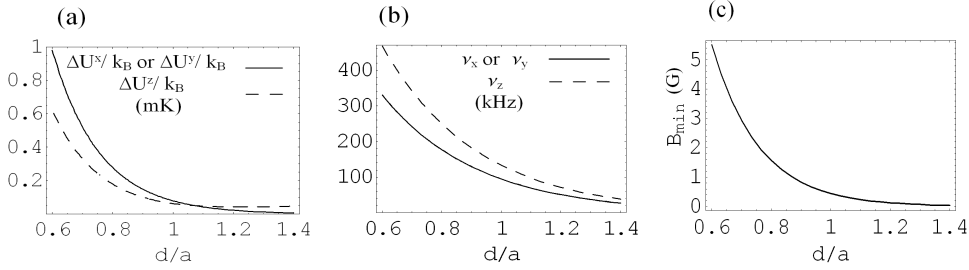


**Figure 6.** Potential barriers (a) and trap frequencies (b) in the  $x$ -,  $y$ - and  $z$ -directions, and  $B_{min}$  (c) for the central minimum, as a function of  $d/a$ , for the parameters given in table 1, column 3.

different values for the barrier heights due to end-effects. The various quantities determined from this calculation are listed in table 2, column 3, along with values determined using the analytical expressions for an infinite symmetrical magnetic lattice with  $B_{1z} = 0$  (column 4) and  $B_{1z} = -0.69$  G (column 5). The values determined from the numerical calculations for the finite lattice with  $B_{1z} = -0.69$  G are in excellent agreement with those determined from the analytical expressions for the infinite, symmetrical lattice with  $B_{1z} = 0$ .

The height of the potential barrier in each direction  $i$  ( $i = x, y, z$ ) for the trapped ultracold atoms is related to the magnetic field barrier height by

$$\Delta U^i = U_{max}^i - U_{min} = m_F g_F \mu_B \Delta B^i \quad (29)$$

The calculated parameters for  $^{87}\text{Rb}$  atoms in the low magnetic field-seeking  $F = 2$ ,  $m_F = +2$  state are listed in column 3 of table 3. The potential barrier heights are  $\Delta U^x = 485 \mu\text{K}$ ,  $\Delta U^y = 486 \mu\text{K}$  and  $\Delta U^z = 307 \mu\text{K}$ , and the trap frequencies are  $\omega_x = 2\pi \times 232 \text{ kHz}$ ,  $\omega_y = 2\pi \times 233 \text{ kHz}$  and  $\omega_z = 2\pi \times 329 \text{ kHz}$ . The trap frequencies may be scaled down, if necessary, by reducing  $c_0 = B_{0x}/B_{0y}$  or  $B_{1x}$  and  $B_{1y}$  [equation(23)].

Figure 5 shows how the distance of the central minimum from the surface,  $d = z_{min} - (t_1 + t_2 + s)$ , expressed in units of the period  $a$ , decreases with increasing strength of the bias magnetic fields  $B_{1x}$  and  $B_{1y}$ . Figure 6(a), (b) and (c) show the exponential increase in magnetic field minimum, potential barrier heights and trap frequencies with decreasing distance  $d$  of the minimum from the surface.

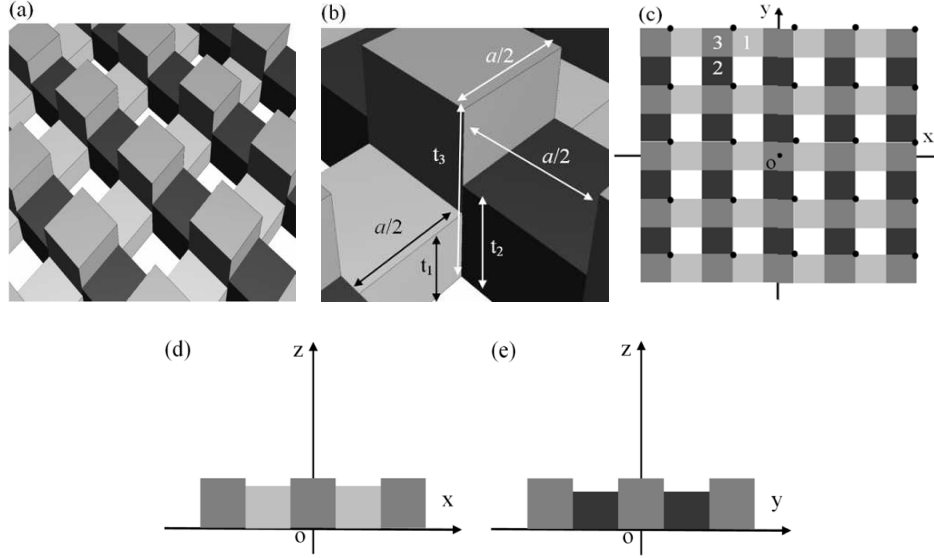


**Figure 7.** Periodic array consisting of one layer of square magnets with three different thicknesses. In (c) the locations of the central minima in the  $x$ - $y$  plane are shown for a symmetrical magnetic lattice with parameters given in table 1, column 4.

Figures 5 and 6 illustrate how the magnetic field minimum, potential barrier heights and the trap frequencies of the microtraps in the magnetic lattice may be controlled by varying the bias magnetic fields  $B_{1x}$  and  $B_{1y}$  to move the microtraps closer to or further from the magnetic array. We note that  $B_{1x}$  and  $B_{1y}$  should be varied simultaneously, according to (16a), while  $B_{1z}$  is constant.

### 3.3. Single layer of periodic arrays of permanent magnets

A second configuration (figure 7), which leads to qualitatively similar 2D magnetic lattices to the two crossed layers of parallel rectangular magnets, but which may be easier to fabricate, consists of a single layer of square-shaped magnets having three different thicknesses plus bias fields in the  $x$ -,  $y$ - and  $z$ -directions, where the thickness of the thickest magnet  $t_3 = t_1 + t_2$ . The parameters used in the numerical calculation are listed in column 4 of table 1 and the quantities determined from this calculation are summarized in the final columns of tables 2 and 3.

## 4. Discussion and summary

Using analytical expressions and numerical calculations we have shown that periodic arrays of permanent magnetic films plus bias magnetic fields can lead to 2D or 1D magnetic lattices of microtraps having *non-zero* potential minima and controllable trap depth. Two configurations have been found that lead to 2D magnetic lattices with non-zero potential minima: the first consists of two crossed layers of periodic arrays of parallel rectangular magnets plus bias fields and the second consists of a single layer of square-shaped magnets having three different thicknesses plus bias fields. These

configurations lead to a *symmetrical* magnetic lattice with equal barrier heights in the  $x$ - and  $y$ -directions in the plane of the array if the bias fields  $B_{1x}$  and  $B_{1y}$  maintain a fixed relationship [given by (16a) or by (16b) for the crossed array configuration] and if the bias field  $B_{1z}$  normal to the array is adjusted to compensate for asymmetry introduced by the finite size of the array. In some experiments, e.g., in studies of quantum tunnelling between lattice sites, it may be useful to be able to vary  $B_{1x}$  and  $B_{1y}$  independently in order to vary the relative barrier heights in the  $x$ - and  $y$ -directions.

For arrays with micron-scale periodicity, the magnetic microtraps can have very large trap depths ( $\sim 0.5$  mK for the parameters chosen for the 2D lattice), allowing relatively warm atoms to be trapped, and very tight confinement. The barrier heights of the microtraps can be controlled by varying the bias fields  $B_{1x}$  and  $B_{1y}$  in the plane of the array, to move the traps either closer to or further from the surface. The numerical calculations for the crossed array configuration were performed for a  $1\text{ mm} \times 1\text{ mm}$  magnetic lattice with period  $a = 1\text{ }\mu\text{m}$ , giving  $10^6$  lattice sites. It should be straight-forward to scale up the magnetic lattice, for example, to a  $1\text{ cm} \times 1\text{ cm}$  lattice with period  $a = 1\text{ }\mu\text{m}$ , giving  $10^8$  lattice sites.

The permanent magnetic lattice configurations considered here should be suitable for trapping and manipulating small clouds of ultracold atoms prepared in low magnetic field-seeking states, including Bose-Einstein condensates and ultracold Fermi gases. A cloud of ultracold atoms could be loaded into the permanent magnetic lattice using, for example, a hybrid magnetic field structure comprising a current-carrying ‘U’ quadrupole trap and a ‘Z’ Ioffe-Pritchard trap located beneath the permanent magnetic array on the atom chip [15]. Such a hybrid structure should allow ultracold atoms to be initially loaded from a mirror MOT into the ‘U’ surface MOT, then into the ‘Z’ magnetic trap, and finally into the 2D magnetic lattice.

By using a small period ( $a \sim 1\text{ }\mu\text{m}$ ) and controlling the barrier height between the microtraps it may be possible to perform quantum tunnelling experiments such as the BEC superfluid to Mott insulator transition [3] in a 2D magnetic lattice. Some of the challenges will include the ability to fabricate permanent magnetic arrays with sufficiently smooth magnetic potentials and *equivalent* magnetic microtraps and to minimise the effects of the interaction of the ultracold atoms with the surface [23, 24, 25, 26, 27, 28, 29] in order to preserve quantum coherence of the atoms in the magnetic lattice. For the magnetic lattices considered here, the potential minima are located about  $1\text{ }\mu\text{m}$  from the surface. At such distances the Casimir Polder force [29] can be significant [27], leading to an attractive component that lowers the barrier height, and losses due to thermally induced spin flips caused by interaction with the ambient temperature surface [25, 26, 27, 28, 29] can be important. However, spin-flip losses can be minimised by using magnetic films whose thickness ( $t \leq 0.4\text{ }\mu\text{m}$  for the magnetic lattices considered here) is much less than the skin depth and by use of suitable dielectric substrates with low electrical conductivity [23]. It should be possible to further reduce interactions with the surface, if necessary, by moving the potential minima further from the surface by decreasing the bias magnetic fields and/or marginally increasing the period of the magnetic lattice. Use of the BEC to Mott insulator transition for ultracold atoms trapped in 2D magnetic lattices could allow the preparation of a single qubit atom on each magnetic lattice site, which is important for scalable quantum information processing.

## Acknowledgments

We thank Romain Pariès for contributions to the early calculations, and Shannon Whitlock, Brenton Hall, Bryan Dalton and Giovanni Modugno for stimulating discussions. This work is supported by a Swinburne University Strategic Initiative Grant. Saeed Ghanbari thanks the Iranian Government for financial support.

## References

- [1] See, for example, Bloch I 2004 *Physics World* **17** 4 25
- [2] Laburthe Tolra B, O'Hara K M, Huckans J H, Phillips W D, Rolston S L and Porto J V 2004 *Phys. Rev. Lett.* **92** 100401
- [3] Greiner M, Mandel O, Esslinger T, Hänsch T and Bloch I 2002 *Nature* **415** 39
- [4] Calarco T, Hinds E A, Jaksch D, Schmiedmayer J, Cirac J I and Zoller P 2000 *Phys. Rev. A* **61** 022304
- [5] Monroe C 2002 *Nature* **416** 238
- [6] Hinds E A and Hughes I G 1999 *J. Phys. D: Appl. Phys.* **32** R119
- [7] Günther A, Kraft S, Kemmler M, Koelle D, Kleiner R, Zimmermann C and Fortágh J (arXiv:cond-mat/0404210)
- [8] Barb I, Gerritsma R, Xing Y T, Goedkoop J B and Spreeuw R J C 2005 *Eur. Phys. J D* **35** 75
- [9] Sinclair C D J, Curtis E A, Retter J A, Hall B V, Llorente-Garcia I, Eriksson S, Sauer B E and Hinds E A 2005 *J Phys: Conf. Series* **19** 74
- [10] Sinclair C D J, Curtis E A, Llorente-Garcia I, Retter J A, Hall B V, Eriksson S, Sauer B E and Hinds E A 2005 *Phys Rev. A* **72** 031603
- [11] Yin J, Gao W, Hu J and Wang Y 2002 *Opt. Commun.* **206** 99
- [12] Grabowski A and Pfau T 2003 *Eur. Phys. J. D* **22** 347
- [13] Wang J Y, Whitlock S, Scharnberg F, Gough D S, Sidorov A I, McLean R J and Hannaford P 2005 *J. Phys. D: Appl. Phys.* **38** 1
- [14] Sidorov A I, McLean R J, Scharnberg F, Gough D S, Davis T J, Sexton B A, Opat G I and Hannaford P 2002 *Acta Phys. Polonica B* **33** 2137
- [15] Hall B V, Whitlock S, Scharnberg F, Hannaford P and Sidorov A 2006 *J. Phys. B: At. Mol. Opt. Phys.* **39** 27
- [16] Sidorov A, Lau D C, Opat G I, McLean R J, Rowlands W J and Hannaford P 1998 *Laser Physics* **8** 642
- [17] Opat G I, Wark S J and Cimmino A 1992 *Appl. Phys. B* **54** 396
- [18] Lau D C, McLean R J, Sidorov A I, Gough D S, Koperski J, Rowlands W J, Sexton B A, Opat G I and Hannaford P 1999 *J. Opt. B* **1** 371
- [19] Opat G I, Nic Chormaic S, Cantwell B P and Richmond J A 1999 *J. Opt. B: Quantum Semiclass. Opt.* **1** 415
- [20] Rosenbusch P, Hall B V, Hughes I G, Saba C V and Hinds E A 2000 *Applied Physics B* **70** 709
- [21] Sidorov A I, McLean R J, Rowlands W J, Lau D C, Murphy J E, Walkiewicz M, Opat G I and Hannaford P 1996 *Quant. Semiclass. Opt.* **8** 713
- [22] Available from: <http://www.esrf.fr/machine/support/ids/public/index.html>
- [23] Henkel C, Pötting S and Wilkens M 1999 *Appl. Phys. B* **69** 379
- [24] Folman R, Krüger P, Schmiedmayer J, Denschlag J and Henkel C, 2002 *Adv. At. Mol. Opt. Phys.* **48** 263
- [25] Jones C, Vale C J, Sahagun D, Hall B V, Eberlein C C, Sauer B E, Furusawa K, Richardson D and Hinds E A 2004 *J. Phys. B: At. Mol. Opt. Phys.* **37** L15
- [26] Harber D M, McGuirk J M, Obrecht J M and Cornell E A 2003 *J. Low Temp. Phys.* **133** 229
- [27] Lin Y, Teper I, Chin C and Vuletić V 2004 *Phys. Rev. Lett.* **92** 050404
- [28] Scheel S, Rekdal P K, Knight P L and Hinds E A 2005 *Phys. Rev. A* **72** 042901
- [29] Casimir H B G and Polder D 1948 *Phys. Rev.* **73** 360